International Astronomy and Astrophysics Research Journal

1(1): 43-57, 2019; Article no.IAARJ.53138

Study of $f(T)$ Dark Energy Model Using Different Choices of the Cosmological Scale Factor

Ayman A. Aly[1], A. Sabry[1*] and M. N. El-Hammamy[1]

[1] *Department of Physics, Faculty of Science, Damnhour University, Damnhour, Egypt.*

Authors' contributions

This work was carried out in collaboration among all authors. All authors read and approved the final manuscript.

Article Information

Editor(s):
(1) Dr. Magdy Rabie Soliman Sanad, Professor, Department of Astronomy, National Research Institute of Astronomy and Geophysics, Cairo, Egypt.
(2) Dr. Hadia Hassan Selim, Professor, Department of Astronomy, National Research Institute of Astronomy and Geophysics, Cairo, Egypt.
Reviewers:
(1) Sarfraz Ali, University of Education, Pakistan.
(2) A. Ayeshamariam, Khadir Mohideen College, India.
(3) Tetiana V. Obikhod, Institute for Nuclear Research NAS of Science, Ukraine.
(4) P. A. Murad, Vienna.
(5) Francisco Bulnes, Tecnológico de Estudios Superiores de Chalco, Mexico.
Complete Peer review History: http://www.sdiarticle4.com/review-history/53138

Received: 08 October 2019
Accepted: 14 December 2019
Published: 24 December 2019

Original Research Article

ABSTRACT

In this paper, we investigated the behaviors of some cosmological parameters as a function of redshift z using some dark energy models namely intermediate, logamediate and emergent scenarios of the universe adopting their cosmological scale factors in the frame work of the teleparallel gravity or the $f(T)$ theory. By considering the present value of cosmological parameters, the behaviors of deceleration, jerk, kerk and lerk parameters and equation of state showed that the universe has an accelerated expansion behavior described by phantom-like behavior. The stability of the model was studied using the squared speed of sound v_s^2 verifying that the model is stable. Finally, we discussed the generalized second law of thermodynamics's (GSLT) validity. The positive behavior of the entropy indicates that the GSLT is verified. These results of functions are in agreement with the recent observational data.

**Corresponding author: E-mail: amanysabry93@gmail.com;*

Keywords: Dark Energy; modified gravity; scale factor; accelerated behavior; inflation.

2010 Mathematics Subject Classification: 53C25, 83C05, 57N16.

1 INTRODUCTION

The universe has an expanded acceleration behavior. The observational data have been obtained for various cosmological experiments of the type Ia supernovae (SNeIa), Large Scale Structure (LSS), X-ray experiments, the Wilkinson Microwave Anisotropy Probe (WMAP), the Planck satellite, the Sloan Digital Sky Survey (SDSS) and Cosmic Microwave Background (CMB) anisotropy radiation, which indicated that our universe has an accelerated expansion behavior [1, 2, 3, 4, 5, 6, 7]. The accelerated expansion represents the present day problems in cosmology. Mainly, a few classes of models exist to explain the accelerated expansion nature of the universe at the present time [8, 9, 10].

Cosmological constant model represents the simplest explanation for the accelerated behavior of the universe and has the Equation of State (EoS) parameter ($\omega_\Lambda = -1$), which should be assumed to clarify the theoretical candidate suggested to explain the observational evidence of accelerated expansion of the universe. We face two main problems described as follows: the fine-tuning and the cosmic coincidence problems [8, 10].

Some theoretical models considered dark energy (DE) as natural dynamic like [11] quintessence ($-1 \leq \omega_\Lambda \leq 1$) [12, 13], phantom ($\omega_\Lambda \leq -1$) [13], Chaplygin gas ($\omega_\Lambda < -1/3$) [14] and k-essence ($\omega_\Lambda < -1/3$) [13]. In fact, some models of dark energy based on the holographic principle [15] that is described by two different types of holographic [8, 10, 16] and agegraphic dark energy [17]. Another interesting suggestions to DE mysterious is the modified gravity which was proposed after the failure of general relativity (GR). GR is considered a very successful theory used to understand the accelerated expansion behavior of the universe [18, 19]. GR is a new set of gravity theories that passes many tests of solar system and astrophysical successfully [20]. The modified gravity theories are important for the late accelerated expansion of the universe which has been studied before by many authors [8]. Some of the familiar models of the modified gravity are $f(T)$, $f(R)$ and $f(G)$, where T is the torsion scalar, R is the Ricci scalar curvature and G is the Gauss-Bonnet invariant [9, 10, 21, 22].

In the present work, we studied the $f(T)$ modified gravity which represents an alternative theory for GR, defined on the Weitzen-bock non-Riemannian manifold which works only with torsion. This model is constructed by Einstein to make an unification inter the electromagnetism and gravity [20]. The $f(T)$ is a general form of the modified teleparallel gravity (TG), where $f(T) = T$ [18, 19, 23, 24].

We investigate the modified $f(T)$ gravity models of dark energy using three different scale factors. We determine some cosmological parameters to explain the acceleration behavior of the universe. Finally, we compare our results with present observations obtained at varying time points. The paper is organized in the following sections. In section 2, we study the modified gravity model of $f(T)$. In section 3, we define three various scenarios of the scale factors. We investigate the accelerated expansion behavior of the universe using the cosmological parameters are defined in section 4, the EoS parameter is represented in section 5, checking the stability of model in section 6 and the validity of the GSLT, which is presented in section 7. Finally, The results are discussed in section 8.

2 THE MODEL

In the framework of $f(T)$ theory, the action S is represented by [25]:

$$S = \frac{1}{16\pi G_N} \int \sqrt{-g} d^4x (f(T) + L_m), \quad (2.1)$$

where G_N indicates the Newton's gravitational constant, g is the determinant of the metric tensor, $f(T)$ is general differentiable function of the torsion and L_m is the Lagrangian density of the matter inside the universe.

According to Eq.(2.1), the action S of a homogeneous and isotropic universe is described from the geometrical point of view,

the Friedmann Lemaitre Robertson Walker (FLRW) model is represented by the Friedman-Robertson-Walker (FRW) metric [26]:

$$ds^2 = -dt^2 + a^2(t)(\frac{dr^2}{1-kr^2} + r^2(d\theta^2 + \mathrm{Sin}^2(\theta)d\varphi^2)), \quad (2.2)$$

where $a(t)$ represents the scale factor, r indicates the radial component of FRW metric and t is the cosmic time. Furthermore, the term of $r^2(d\theta^2 + \mathrm{Sin}^2(\theta)d\varphi^2)$ is the solid angle element squared and the quantities θ and φ are the usual azimuthal and polar angles that are assumed in the range of $0 \leq \theta \leq \pi$ and $0 \leq \varphi \leq 2\pi$ [16].

The expansion factor of the universe can be assumed as a Taylor series at the present time t_o [26]:

$$a(t) = a_o(1 + \sum_{n=1}^{\infty} \frac{A_n(t_o)}{n!}(H_o(t - t_o))^n), \quad (2.3)$$

where $A_n = \frac{a^{(n)}}{aH^n}$, $n \in N$ and $a^{(n)}$ is the n^{th} derivative of the scale factor with respect to the time scale [15, 26].

In this work, we construct the $f(T)$ form which includes constant, linear and non-linear of torsion T, is given by [9, 20],

$$f(T) = T + \frac{6(n-1)^u}{u-1}(-\frac{T}{6n^2})^{u/2} + \frac{\sqrt{-T}}{\sqrt{6}n}, \quad (2.4)$$

where u, n are constants and T is the torsion scalar [10]. Different ranges of n indicate different epoch of the evolution of universe such as $0 < n \leq 1$ and $n = \frac{2}{3}$ represent radiation and matter dominated decelerated phases. The accelerated behavior is realized when $n > 1$ [9]. The Hubble parameter is $H = \frac{n}{t}$ and the torsion scalar is assigned to [9]:

$$T(t) = -6H^2 = \frac{-6n^2}{t^2}. \quad (2.5)$$

The Hubble horizon is taken as the infrared (IR) cut-off, while the holographic dark energy density is found to be [10] :

$$\rho_\Lambda = 3c^2 M_p^2 L^{-2}, \quad (2.6)$$

where $M_p = (8\pi G_N)^{-\frac{1}{2}} \approx 10^{18}\ GeV$ indicates the reduced Planck mass and L is the IR cut-off size [27]. Gao et al. [28] took the Ricci scalar as an IR cut-off, where the Ricci dark energy is proportional to the Ricci scalar [27]. The Ricci scalar curvature of FLRW universe is appointed [10]:

$$R = -6\left(\dot{H} + 2H^2 + \frac{k}{a^2}\right), \quad (2.7)$$

where k is the curvature parameter, which can be ∓ 1 and 0, respectively, yielding an open, a closed, or a flat FRW universe. Let us consider DE component is proportional to the inverse of squared Ricci scalar curvature radius as described in the holographic principle term [28], where energy density ρ of Ricci dark energy (RDE) model for a flat FLRW universe is given by, for $k = 0$ [10],

$$\rho = 3c^2\left(\dot{H} + 2H^2\right). \quad (2.8)$$

By differentiating Eq.(2.8), the time derivative of dark energy density is described by [10]:

$$\dot{\rho} = 3c^2\left(\ddot{H} + 4\dot{H}H\right), \quad (2.9)$$

where c^2 is a positive constant.

3 DIFFERENT SCENARIOS OF THE SCALE FACTORS

3.1 Intermediate Inflation

The expansion of universe is expressed in exponential form. The intermediate expansion scale factor is defined as [29, 30]:

$$a = e^{\mathrm{Bt(z)}^n}, \quad (3.1)$$

where $B > 0$ and $0 < n < 1$.

3.2 Logamediate Inflation

We investigated another generalized form of inflation, which called 'logamediate inflation'. The scale factor has the form [30]:

$$a = e^{A(\mathrm{Log}t(z))^n}. \quad (3.2)$$

where $A > 0$ and $n > 1$.
We clarified some calculations to the behavior of higher-order characteristics for the logamediate inflation.

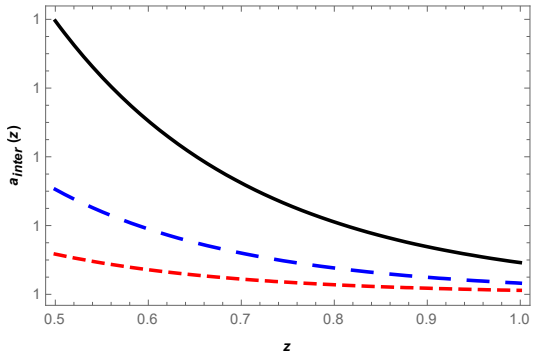

Fig. 1. The behavior of $a_{inter}(z)$ as a function of z for the intermediate inflation, for $n = 5$ (black-solid), $n = 5.2$ (blue-dashed) and $n = 5.4$ (red-dashed)

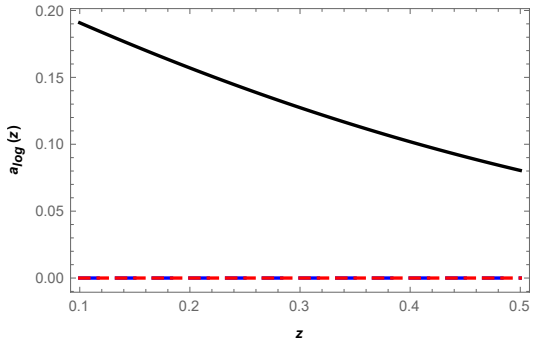

Fig. 2. The behavior of $a_{log}(z)$ as a function of z for the logamediate inflation, for $n = 5$ (black-solid), $n = 7$ (blue-dashed) and $n = 9$ (red-dashed)

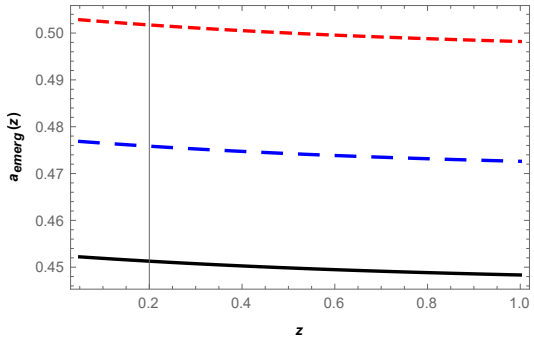

Fig. 3. The behavior of $a_{emerg}(z)$ as a function of z for the emergent inflation, for $n = 5$ (black-solid), $n = 5.2$ (blue-dashed) and $n = 5.4$ (red-dashed)

3.3 Emergent Inflation

The Emergent Inflation presents a framework of discussions for suggestions if whatever process caused the universe to come into being, preferred the high-symmetry state of the Einstein static model to any less ordered state [31]. For the emergent universe, the scale factor can be chosen as [32]:

$$a = a_o \left(\lambda + e^{\mu t(z)}\right)^n, \tag{3.3}$$

where a_o, λ, μ and n are positive constants [10, 33],

1. $a_o > 0$ for the scale factor a to be positive.
2. $a > 0$ or $n > 0$ for expanding model of the universe.
3. $a < 0$ and $n < 0$ imply big bang singularity at $t = -\infty$.
4. $\lambda > 0$ to avoid any uniqueness at finite time (big rip).

In the next sections, we are going to establish the expressions of some cosmological parameters that is necessary to describe the behavior of the considered different scenarios of scale factors.

4 COSMOLOGICAL PARAMETERS

The higher-order characteristics of the universe could be related to the accelerated expansion behavior.

The Hubble parameter is derived from [15, 34]:

$$H = \frac{\dot{a}}{a}. \tag{4.1}$$

The deceleration parameter is given by [15]:

$$q = -\frac{1}{H^2}\frac{\ddot{a}}{a}. \tag{4.2}$$

The jerk parameter is [15]:

$$j = \frac{1}{H^3}\frac{\dddot{a}}{a}. \tag{4.3}$$

The kerk or snap parameter is [15]:

$$\kappa = -\frac{a^4}{aH^4}. \tag{4.4}$$

The lerk parameter is [15]:

$$l = \frac{1}{H^5}\frac{a^{[5]}}{a}. \tag{4.5}$$

The general form of these parameters which is denoted by x^i can be expressed by [34]:

$$x^i = \frac{(-1)^{i+1}a^i}{aH^i} = (-1)^{i+1}\frac{a^i a^{i-1}}{\dot{a}^{i+1}}. \tag{4.6}$$

where i-th indicates the order of the derivative with respect to the cosmic time t and i is just a power. Eq.(4.2) is the universal acceleration can be quantified through a dimensionless cosmological function. For $q < 0$, it describes the accelerated universe. While for $q \geq 0$, it is simplified for either decelerated or expanded universe at $a \propto t$. The dimensionless third time derivative of the scale factor with respect to cosmic time is defined in Eq.(4.3), it is known as "jerk parameter" and also "statefinder parameter". Eq.(4.4) has the fourth time derivative of scale factor. While Eq.(4.5) is the fifth time derivative of scale factor [15, 34].

It's well known that the relation between cosmic time and redshift z is [35]:

$$t(z) = \frac{2}{((z+1)^2+1)\,H_o}. \tag{4.7}$$

The present time t_o at $z = 0$ can be obtained from the relation:

$$t_o = \frac{1}{H_o}. \tag{4.8}$$

4.1 Intermediate Inflation

Adopting Eq.(4.2), Eq.(4.3), Eq.(4.4) and Eq.(4.5) for the intermediate inflation, we obtain these behaviors as shown in Fig. 4:

In Fig. 4, we represent the evolution of q, j, κ and l for different values of n. In Fig. 4a, we notice that the deceleration parameter (q) has a slight decreasing behavior at negative level ($q < 0$) for all n values. Consequently, this result indicates that our universe is in continuous accelerating expansion.

Fig. 4b shows that the jerk parameter (j) has a positive increasing behavior against the redshift z for three values of n. For $n = 5$, the jerk parameter is $j \simeq 4.17349 \times 10^{19}$ at $z \sim 0.05$ and $j \simeq 6.53741 \times 10^{19}$ at $z \sim 0.1$, showing a slow increasing behavior.

Fig. 4c displays the kerk parameter (κ) which has a negative decreasing behavior for all values of n. For $n = 5$, the black-solid line from $\kappa_{z=0.05} \simeq -3.56705 \times 10^{30}$ to $\kappa_{z=0.1} \simeq -7.16964 \times 10^{30}$ tends to be a constant rate of deceleration. Adopting $n = 5.2$ (blue-dashed) and $n = 5.4$ (red-dashed), we notice a decreasing behavior for $\kappa < 0$.

As evident from Fig. 4d that the lerk parameter (l) has an increasing behavior at positive level. For $n = 5$, we find the black-solid line from $l_{z=0.05} \simeq 2.03249 \times 10^{41}$ to $l_{z=0.1} \simeq 5.242 \times 10^{41}$ tends to be $zero$. For $n = 5.2$ (blue-dashed) and $n = 5.4$ (red-dashed), the behavior is found to be increased for $l > 0$.

4.2 Logamediate Inflation

The behaviors of the cosmological parameters are presented in Fig. 5:

The parameters q, j, κ and l that expressed in Fig. 5 versus the red-shift z. We notice from Fig. e that a decreasing behavior at negative level as obtained from SNela data for all n values. The negative level of $q < 0$ indicates the universe has an accelerated behavior and from $q_{z=1} \simeq -0.524361$ to $q_{z=3} \simeq -0.812034$ show a slowly decreased behavior.

Fig. f has an increasing behavior ($j > 0$) for three values of n. Values of $n = 7$ (blue-dashed) and $n = 9$ (red-dashed) show a tiny increased behavior and tend to be constant.

In Fig. g, we obtain a decreasing behavior remains negative ($-1 < \kappa < 0$) for all values of n. Fig. h displays an increasing behavior at positive level for the values of $n = 7$ (blue-dashed) and $n = 9$ (red-dashed), i.e., $l > 0$. For the value of $n = 5$ (black-solid), the behavior decreases from $l_{z=1} \simeq -0.000199579$ to $l_{z=2} \simeq -8.85769 \times 10^{-6}$ and begins in increasing at $l_{z\simeq 2.1} \simeq 5.09981 \times 10^{-7}$.

4.3 Emergent Inflation

The cosmological parameter in Fig. 6 has the following behaviors:
The evolution of q, j, κ and l parameters as a functions of red-shift z is shown in Fig. 6. From Fig. i, we notice a very small decreasing behavior where $q < 0$, indicating a continuous accelerating behavior of the universe.

For the jerk parameter in Fig. j, we also have an increasing behavior for three values of n.
Fig. k presents a negative decreasing behavior, where $\kappa < -1$ for all positive values of n.

The behavior of l parameter as a function of redshift z in Fig. l is increasing at positive level, i.e., $l > +1$ for different values of n, from $z = 0$ to $z = 4$.

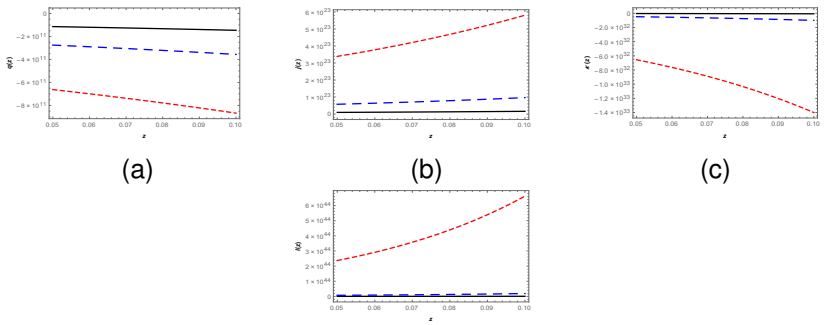

(a) (b) (c)

(d)

Fig. 4. The behavior of (a) deceleration, (b) jerk, (c) kerk and (d) lerk parameters as a function of red-shift z for the intermediate inflation, for $n = 5$ (black-solid), $n = 5.2$ (blue-dashed) and $n = 5.4$ (red-dashed)

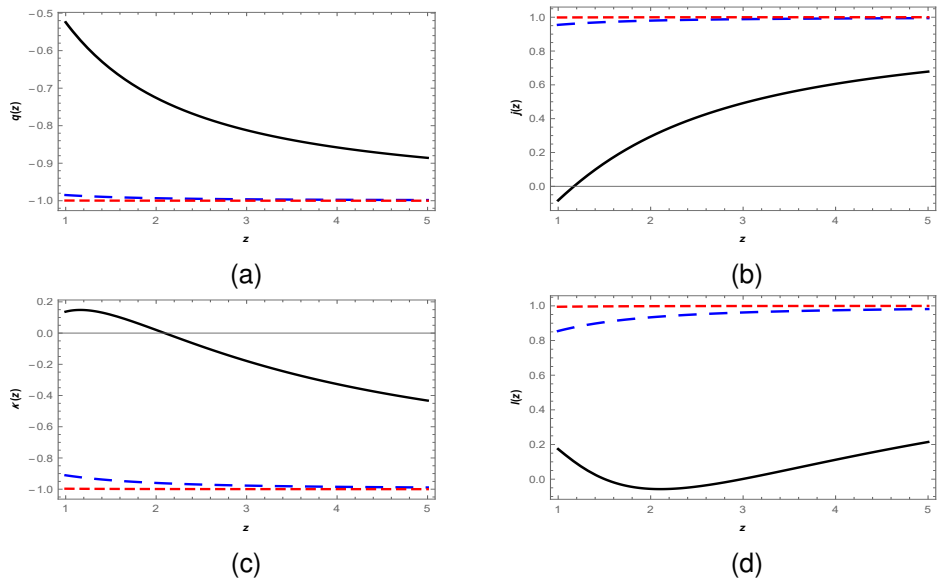

Fig. 5. The behavior of (e) deceleration, (f) jerk, (g) kerk and (h) lerk parameters as a function of red-shift z for logamediate inflation when $n = 5$ (black-solid), $n = 7$ (blue-dashed) and $n = 9$ (red-dashed)

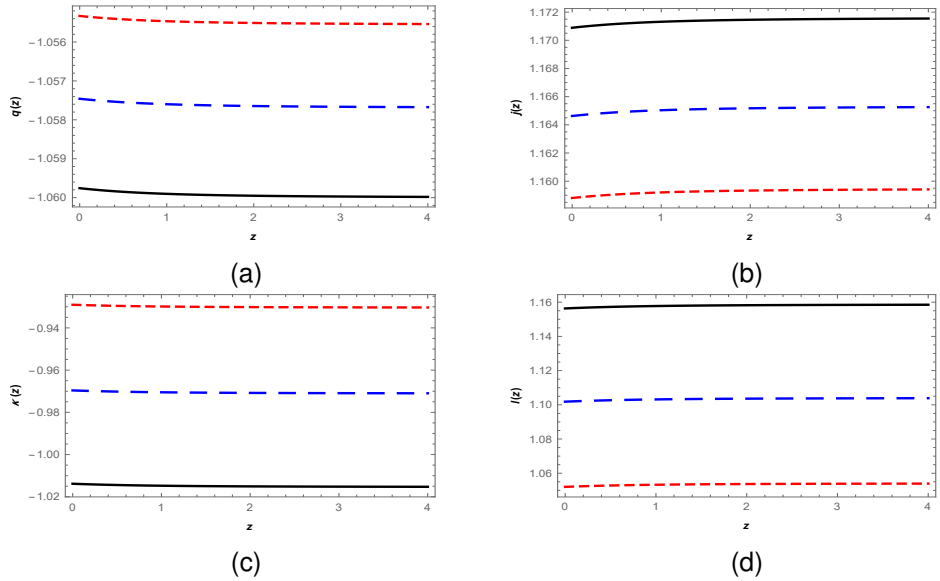

Fig. 6. The behavior of (i) deceleration, (j) jerk, (k) kerk and (l) lerk parameters as a function of z for the emergent inflation, for $n = 5$ (black-solid), $n = 5.2$ (blue-dashed) and $n = 5.4$ (red-dashed)

5 THE EQUATION OF STATE PARAMETER

We derive the expression of EoS parameter for the non-interacting and the interacting DE. We start considering the non-interacting case.

The continuity equations are given by [36]:

$$\dot{\rho_{\text{tot}}} + 3\text{H}\rho_{\text{tot}}\left(\omega_{\text{tot}} + 1\right) = 0, \tag{5.1}$$

where ω_{tot} is the total EoS parameter. If there is no interaction between DE sectors, the two energy densities ρ and ρ_{m} of DE and dark matter (DM) are derived as [36]:

$$\dot{\rho} + 3\text{H}\rho\left(\omega_{\Lambda} + 1\right) = 0, \tag{5.2}$$

$$\dot{\rho}_m + 3H\rho_m = 0, \tag{5.3}$$

where ω_{Λ} is the EoS parameter of DE and the EoS parameter of DM is $\omega_{\text{m}=0}$ due to $p_{\text{m}} = 0$.

Inserting Eq.(2.8) and Eq.(2.9) in Eq.(5.2), we obtain the non-interacting EoS parameter $\omega_{\Lambda non}$:

$$\omega_{\Lambda non} = -\frac{\left(\ddot{H} + 4\dot{H}H\right)}{3H\left(\dot{H} + 2H^2\right)} - 1. \tag{5.4}$$

For the interacting case, the continuity equations are expressed as [36]:

$$\dot{\rho} + 3\text{H}\rho\left(\omega_{\Lambda} + 1\right) = -Q, \tag{5.5}$$

$$\dot{\rho}_m + 3H\rho_m = Q, \tag{5.6}$$

where Q is an arbitrary function of cosmological parameters, called the interaction term and is chosen here as $Q = 3\delta H\rho_m$ [10, 16], where δ is the dimensionless coupling between DE and DM and is known as a transfer strength or an interaction parameter. The cosmological observational data obtained from different cosmological experiments determined the coupling parameter between DM and DE, that must be assumed to be small positive value and be in agreement with the experiments. Observations of CMB radiation suggest that the interaction term is $0 < \delta < 0.025$. This result is consistent with the interaction term δ must be taken in the range of $(0, 1)$ in the limiting case of $\delta = 0$ which leads to the non-interacting model [16].

By solving the continuity equation for ρ_m, see Eq.(5.6), the energy density of DM is defined as [10]:

$$\rho_m = \rho_{\text{mo}} a^{-3(1+\delta)}, \tag{5.7}$$

where ρ_{mo} indicates the present time value of ρ_m. Adopting Eq.(2.8) and Eq.(2.9) in Eq.(5.5), the interacting EoS parameter $\omega_{\Lambda inter}$ is expressed as follows:

$$\omega_{\Lambda inter} = -\frac{\delta\rho_m}{\rho} - \frac{\left(\ddot{H} + 4\dot{H}H\right)}{3H\left(\dot{H} + 2H^2\right)} - 1. \tag{5.8}$$

5.1 Intermediate Inflation

The behavior of EoS parameter for both cases of non-interacting and interacting DE for the intermediate inflation is expressed in Fig. 7:

Fig. 7 presents the variation of EoS parameter for non-interacting and interacting cases versus redshift z. It is seen from Fig. m and Fig. n that the EoS parameter is in a decreasing negative behavior which indicates a phantom-like behavior for different values of n, over the considered range of redshift.

5.2 Logamediate Inflation

In Fig. 8, the behaviors of non-interacting and interacting EoS parameter of the logamediate inflation are considered as:

Fig. o has a decreasing behavior at negative level $\omega_{\Lambda non} > -1$, i.e., the non-interacting case is in a phantom-like behavior, for n values, $n = 5$ (black-solid), $n = 7$ (blue-dashed) and $n = 9$ (red-dashed).

Fig. p represents a negative decreasing behavior for $n = 7$ where the blue-dashed line for $\omega_{\Lambda inter, z=0.01} \simeq -0.947018$ indicates a phantom-like behavior. For $n = 5$, the black-solid line from $\omega_{\Lambda inter, z=0.01} \simeq 0.112782$ to $\omega_{\Lambda inter, z=0.05} \simeq 0.0677319$ shows a quintessence phase, from $z = 0.01$ to $z = 0.05$.

5.3 Emergent Inflation

The behaviors of the EoS parameter for both non-interacting and interacting emergent inflation are expressed in fig. 9:

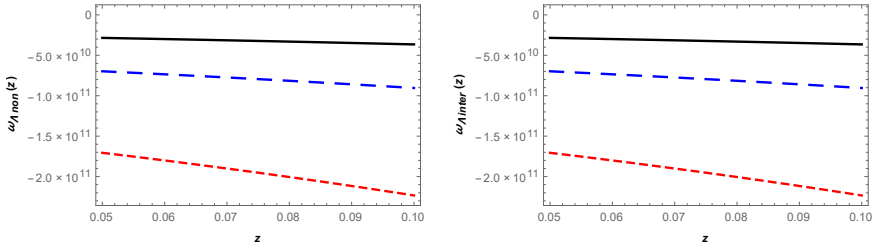

(a) (b)

Fig. 7. The behavior of EoS parameter as a function of red-shift z for the (m) non-interacting and (n) interacting intermediate inflation, for $n = 5$ (black-solid), $n = 5.2$ (blue-dashed) and $n = 5.4$ (red-dashed)

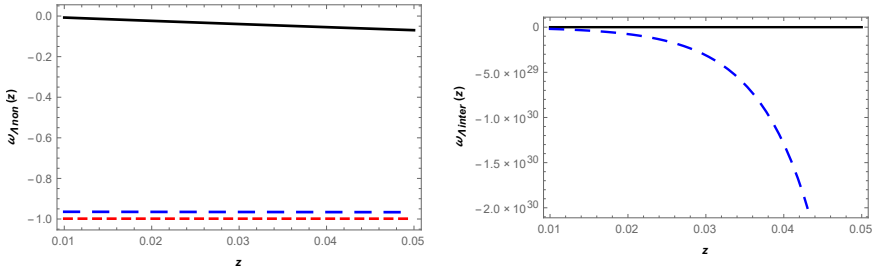

(a) (b)

Fig. 8. The behavior of EoS parameter as a function of red-shift z for the (o) non-interacting (p) interacting logamediate inflation for $n = 5$ (black-solid), $n = 7$ (blue-dashed) and $n = 9$ (red-dashed)

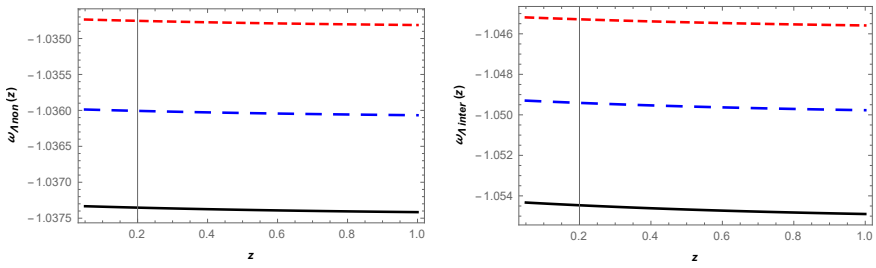

(a) (b)

Fig. 9. The behavior of EoS parameter as a function of red-shift z for the (q) non-interacting (r) interacting emergent inflation for $n = 5$ (black-solid), $n = 5.2$ (blue-dashed) and $n = 5.4$ (red-dashed)

In Fig. q, the EoS parameter is a function of redshift z and $\omega_{\Lambda non} < -1$ indicates a decreasing negative behavior. We also notice a decreasing behavior in Fig. r. The EoS for both cases of DE does not cross the phantom barrier $(\omega_\Lambda < -1)$ and the model does not exhibit a quintessence-like behavior for various values of $n = 5$ (black-solid), $n = 5.2$ (blue-dashed) and $n = 5.4$ (red-dashed), over the considered range of redshift.

The pressure (P) of DE could be defined by using the scalar field and the interactions between DE and DM as [10]:

$$p = \frac{\gamma}{2}(\dot{\phi})^2 - V(\phi(t)) + 16Hf'(\phi(t))\frac{\ddot{a}}{a} + 8H^2\left(f'(\phi(t))\ddot{\phi} + f''(\phi(t))\left(\dot{\phi}\right)^2\right), \quad (5.9)$$

where the scalar field is given by $\phi(t) = a(t)^n\phi_o$ and ϕ_o is a positive constant. The prime indicates a derivative with respect to ϕ [10]. Here $f'(\phi) = \frac{df}{d\phi}$ and $f''(\phi) = \frac{d^2f}{d\phi^2}$ [9, 10].

The total energy density of DE and DM $\rho + \rho_m$ is [10]:

$$\rho + \rho_m = \frac{\gamma}{2}(\dot{\phi})^2 + V(\phi) - 24H^3f'(\phi)\dot{\phi}. \quad (5.10)$$

The potential of the interacting DE is given by solving Eq.(5.10) [10]:

$$V(\phi(t)) = \rho_m + \rho - \frac{\gamma}{2}\left(\dot{\phi}\right)^2 + 24\dot{f}(\phi(t))\dot{\phi}H^3. \quad (5.11)$$

To reconstruct the potential of the interacting DE as a function of the cosmic time t, we solve Eq.(2.8) with Eq.(5.7) in Eq.(5.11), then [10]:

$$V(\phi(t)) = \rho_{\text{mo}}a^{-3(1+\delta)} + 3c^2\left(\dot{H} + 2H^2\right) - \frac{\gamma}{2}\left(\dot{\phi}\right)^2 + 24f'(\phi(t))\dot{\phi}H^3. \quad (5.12)$$

6 SQUARED SPEED OF THE SOUND

Let us study an important parameter in cosmology which is used to check the stability of any DE model. This quantity is known as 'squared speed of sound' v_s^2.
The general definition is assigned as [16, 37]:

$$v_s^2 = \frac{\dot{p_{\text{tot}}}}{\dot{\rho_{\text{tot}}}} = \frac{\dot{p}}{\dot{\rho} + \dot{\rho_m}}, \quad (6.1)$$

where $p_{\text{tot}} = p$ is the total pressure and $\rho_{\text{tot}} = \rho_m + \rho_{\text{mo}}$ is the total energy density of the DE model. The sign of v_s^2 plays an important role in determining the stabilization of DE model. If $v_s^2 < 0$, it means that the model is unstable. Moreover, if $v_s^2 > 0$, the model is stable [37].

6.1 Intermediate Inflation

The v_s^2 behavior is presented in Fig.10:

The behavior of squared speed of sound parameter for different values of n is shown in Fig. 10. We find a decreased function remains positive when $n = 5$ (black-solid) and $n = 5.2$ (blue-dashed) at the considered range from $z = 0.05$ to $z = 0.1$. This result indicates the stability of the model when $v_s^2 > 0$.

6.2 Logamediate Inflation

The behavior of v_s^2 is revealed in Fig. 11:

In Fig. 11, the behavior of $v_s^2(z)$ as a function of redshift z in case of logamediate expansion. It represents an increasing behavior at positive level for $n = 5$ (black-solid) and this is from $z = 0.01$ to $z = 0.05$. The stability behavior of universe happens when $v_s^2 > 0$, independently on the values of n.

6.3 Emergent Inflation

The behavior of v_s^2 is expressed in Fig. 12:

Fig.12 clarifies an increasing positive behavior for all values of n, so $v_s^2 > 0$ represents the stability of the model.

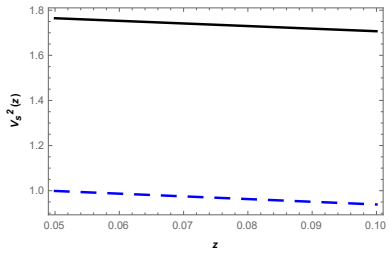

Fig. 10. The behavior of $v_s^2(z)$ as a function of red-shift z for the intermediate inflation for $n = 5$ (black-solid), $n = 5.2$ (blue-dashed) and $n = 5.4$ (red-dashed)

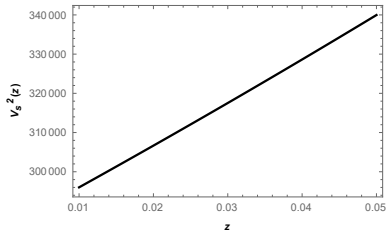

Fig. 11. The behavior of $v_s^2(z)$ as a function of red-shift z for the logamediate inflation, for $n = 5$ (black-solid)

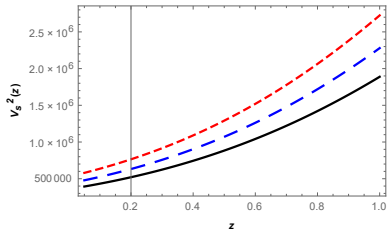

Fig. 12. The behavior of $v_s^2(z)$ as a function of red-shift z for the emergent inflation for $n = 5$ (black-solid), $n = 5.2$ (blue-dashed) and $n = 5.4$ (red-dashed)

7 GENERALIZED SECOND LAW OF THERMODYNAMICS

Bekenstein and Hawking determined that the entropy of black hole is proportional to its event horizon [38] which leads to GSLT for black hole physics. This law can be defined as the entropy of black hole and its area is always increasing. According to GSLT, the entropy of horizon and entropy of matter sources inside horizen does not decrease with respect to time.

$$\frac{dS_{\text{horizon}}}{dt} + \frac{dS_{\text{inside}}}{dt} \geq 0, \tag{7.1}$$

$$\dot{S}_{\text{tot}} = \dot{S}_h + \dot{S}_{\text{in}} \geq 0, \tag{7.2}$$

where $\dot{S}_h$ is the entropy of horizon and $\dot{S}_{\text{in}}$ is the entropy of matter inside horizon.

7.1 Entropy of Matter Inside Horizon

From Gibb's equation, we have [39]

$$T_{\text{emp}} dS_{\text{in}} = P_{\text{eff}} dV_{\text{ol}} + dE_{\text{in}}. \tag{7.3}$$

The IR cut-off of the universe R_h is equal to the apparent horizon [39]:

$$R_h = \frac{1}{H}, \tag{7.4}$$

and the temperature inside the horizon is evidenced as follow [39]:

$$T_{\text{emp}} = \frac{1}{2\pi R_h}. \tag{7.5}$$

The volume of the system is [39]:

$$V_{\text{ol}} = \frac{4\pi}{3} R_h^2. \tag{7.6}$$

The internal energy of system is [39]:

$$E_{\text{in}} = \rho_{\text{eff}} V_{\text{ol}}. \tag{7.7}$$

Now, one can put Eq.(7.4), Eq.(7.5), Eq.(7.6) and Eq.(7.7) together in Eq.(7.3) to obvious the following relation:

$$\dot{S}_{\text{in}} = 8\pi^2 R_h^3 \left(\rho_m - \frac{\dot{\rho}}{3H}\right)\left(\dot{R}_h - 1\right). \tag{7.8}$$

7.2 Bekenstein Entropy

Gibbons and Hawking developed the idea of Bekenstein for cosmological system, where the entropy of cosmological event horizon is proportional to horizon area. It is afforded as [39]:

$$S_h = \frac{A_B}{4G}. \tag{7.9}$$

The Bekenstein equation (7.9) relates qualitatively various quantities: a geometric quantity on the right hand side, the area A_B of a black hole and an information theoretic quantity on the left hand side, the entropy S_h of the black hole [40]. From the relation, $A_B = 4\pi R_h^2$ and $G = 1$, one obtains:

$$S_h = \pi R_h^2, \tag{7.10}$$

$$\dot{S}_h = 2\pi R_h \dot{R}_h. \tag{7.11}$$

Finally, by inserting Eq.(7.8) with Eq.(7.11) in Eq.(7.2), we get [39]:

$$\dot{S_{\text{tot}}} = 8\pi^2 R_h^3 \left(\rho_m - \frac{\dot{\rho}}{3H}\right)\left(\dot{R}_h - 1\right) + 2\pi R_h \dot{R}_h. \tag{7.12}$$

7.2.1 Intermediate inflation

The behavior of total entropy performs in Fig. 13:

In Fig. 13, the behavior of $\dot{S_{\text{tot}}}(z)$ as a function of redshift z in case of intermediate expansion. We have an increasing behavior at positive level ($\dot{S_{\text{tot}}}(z) > 0$) for $n = 3$ (red-dashed), but for other values of n, $n = 1$ (black-solid) and $n = 2$ (blue-dashed) the behavior of $\dot{S_{\text{tot}}}(z) = 0$, from $z = 0.05$ to $z = 1$.

7.2.2 Logamediate inflation

The total entropy is expressed in Fig. 14:

In Fig. 14, the behavior of $\dot{S_{\text{tot}}}(z)$ as a function of redshift z for the logamediate expansion. We notice an increasing positive behavior for $n = 7$ (blue-dashed), but for $n = 5$ (black-solid), the behavior of $\dot{S_{\text{tot}}}(z) = 0$, over the considered range of redshift.

7.2.3 Emergent inflation

The behavior of total entropy is realized in Fig. 15:

Fig. 15 presents an increasing behavior at positive level, where $\dot{S_{\text{tot}}}(z) > 0$ for all values of n from $z = 0.05$ to $z = 1$.

For three cases, we have an increasing positive behavior. $\dot{S_{\text{tot}}}(z) > 0$ indicates the GSLT is verified.

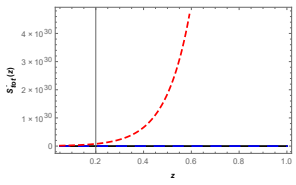

Fig. 13. The behavior of $\dot{S_{\text{tot}}}(z)$ for the intermediate inflation for $n = 1$ (black-solid), $n = 2$ (blue-dashed) and $n = 3$ (red-dashed)

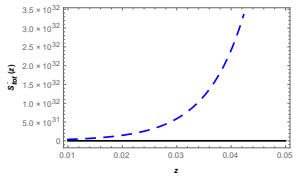

Fig. 14. The behavior of $\dot{S_{\text{tot}}}(z)$ for the logamediate inflation for $n = 5$ (black-solid), $n = 7$ (blue-dashed) and $n = 9$ (red-dashed)

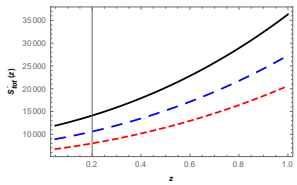

Fig. 15. The behavior of $\dot{S_{\text{tot}}}(z)$ for the emergent inflation for $n = 5$ (black-solid), $n = 5.2$ (blue-dashed) and $n = 5.4$ (red-dashed)

8 CONCLUSIONS

In this paper, the $f(T)$ model is considered for different scale factor scenarios to explain the cosmological accelerated expansion behavior of the universe. In each model of our study, we used different values of physical parameters as: for the intermediate inflation, the values of physical parameters are $u = -2$, $B = 0.02$, $\phi_o = 0.14$, $\rho_{\text{mo}} = 0.23$, $\delta = 0.05$, $z_o = 1$ and $H_o = 74$. For the logamediate inflation, $A = 10^{-3}$,$\phi_o = 0.14$, $\rho_{\text{mo}} = 0.23$ and $\delta = 0.05$. For the emergent inflation, $a_o = 0.12$, $\mu = 0.3$, $\lambda = 0.3$, $\phi_o = 0.14$, $\rho_{\text{mo}} = 0.23$ and $\delta = 0.05$.

a In the section (4), the characteristics of the universe represented by the deceleration parameter q, the jerk parameter j, the kerk parameter κ and the lerk parameter l. The negative value of q describes the accelerated expansion of the universe, while the value of jerk parameter is helpful for distinguishing the different accelerating models, also j can indicate the dynamics of the universe acceleration. The kerk parameter κ and the lerk parameter l indicate that the universe has an accelerating behavior.

b In the section (5), the behavior of the EoS parameter of DE is studied for both non-interacting and interacting DE sectors. We notice that the values of the ΛCDM model can be assumed to be greater, equals or less than -1. Assuming $-1 \leq \omega_\Lambda \leq 1$ indicates quintessence-like behavior, and for $\omega_\Lambda \leq -1$ represents phantom-like behavior. In Figs.7, 8 and 9 the EoS parameter has a decreasing behavior for both $\omega_{\Lambda non}$ and $\omega_{\Lambda inter}$ at negative part that indicates a phantom-like behavior.

c In the section (6), the squared speed of the sound determines if the model is stable or not. We notice that the model is either stable or unstable depending on the values of the parameters. In Figs. 10, 11 and 12, the $v_s^2 > 0$ indicates a stable DE model.

d In the section (7), the GSLT proves the validity of thermal entropy and the increasing behavior of the black-hole's entropy refers to $\dot{S_{\text{tot}}}(z) > 0$.

These results are in agreement with the observed data which proved that our model in the framework of $f(T)$ modified gravity leads to an accelerated universe.

COMPETING INTERESTS

Authors have declared that no competing interests exist.

REFERENCES

[1] Perlmutter S, Aldering G, Goldhaber G, Knop R, Nugent P, Castro P, et al. Measurements of Ω and Λ from 42 high-redshift supernovae. The Astrophysical Journal. 1999;517(2):565.

[2] Spergel DN, Bean R, Doré O, Nolta M, Bennett C, Dunkley J, et al. Three-year Wilkinson Microwave Anisotropy Probe (WMAP) observations: implications for cosmology. The Astrophysical Journal Supplement Series. 2007;170(2):377.

[3] Spergel DN, Verde L, Peiris HV, Komatsu E, Nolta M, Bennett C, et al. First-year Wilkinson Microwave Anisotropy Probe (WMAP)* observations: determination of cosmological parameters. The Astrophysical Journal Supplement Series. 2003;148(1):175.

[4] Contaldi CR, Hoekstra H, Lewis A. Joint CMB and weak lensing analysis; physically motivated constraints on cosmological parameters; 2003. arXiv preprint astro-ph/0302435.

[5] Colless M, Dalton G, Maddox S, Sutherland W, Norberg P, Cole S, et al. The 2df galaxy redshift survey: spectra and redshifts. Monthly Notices of the Royal Astronomical Society. 2001;328(4):1039–1063.

[6] Tegmark M, Strauss MA, Blanton MR, Abazajian K, Dodelson S, Sandvik H, et al. Cosmological parameters from SDSS and WMAP. Physical review D. 2004;69(10):103501.

[7] Riess AG, Filippenko AV, Challis P, Clocchiatti A, Diercks A, Garnavich PM, et al. Observational evidence from supernovae for an accelerating universe and a cosmological constant. The Astronomical Journal. 1998;116(3):1009.

[8] Chattopadhyay S, Pasqua A, Aly AA. Interacting Ricci dark energy in scalar Gauss-Bonnet gravity. The European Physical Journal Plus. 2014;129(2):31.

[9] Jawad A, Rani S, Saleem M. Cosmological study of reconstructed $f(T)$ models. Astrophysics and Space Science. 2017;362(4):63.

[10] Pasqua A, Chattopadhyay S, Khurshudyan M, Aly AA. Behavior of Holographic Ricci Dark Energy in Scalar Gauss-Bonnet Gravity for Different Choices of the Scale Factor. International Journal of Theoretical Physics. 2014;53(9):2988–3013.

[11] Tajahmad B. Reconstruction of $F(T)$ gravity in homogeneous backgrounds; 2018. arXiv preprint arXiv:181210339.

[12] Nojiri S, Odintsov SD. Introduction to modified gravity and gravitational alternative for dark energy. International Journal of Geometric Methods in Modern Physics. 2007;4(01):115–145.

[13] Copeland EJ, Sami M, Tsujikawa S. Dynamics of dark energy. International Journal of Modern Physics D. 2006;15(11):1753–1935.

[14] Bilic N, Tupper GB, Viollier RD. Dark matter, dark energy and the Chaplygin gas; 2002.

[15] Ghosh R, Chattopadhyay S, Debnath U. A dark energy model with generalized uncertainty principle in the emergent, intermediate and logamediate scenarios of the universe. International Journal of Theoretical Physics. 2012;51(2):589–603.

[16] Pasqua A, Chattopadhyay S, Beesham A. A look into the cosmological consequences of a dark energy model with higher derivatives of H in the framework of Chameleon Brans-Dicke Cosmology; 2016. arXiv preprint arXiv:160703384.

[17] Karami K, Khaledian M, Felegary F, Azarmi Z. Interacting new agegraphic tachyon, K-essence and dilaton scalar field models of dark energy in non-flat universe. Physics Letters B. 2010;686(4-5):216–220.

[18] Bahamonde S, Camci U. Exact Spherically Symmetric Solutions in Modified Teleparallel gravity. Symmetry. 2019;11(12):1462.

[19] Hohmann M, Järv L, Krššák M, Pfeifer C. Modified teleparallel theories of gravity in symmetric spacetimes; 2016. arXiv preprint arXiv:190105472.

[20] Jamil M, Momeni D, Myrzakulov R. Attractor solutions in f (T) cosmology. The European Physical Journal C. 2012;72(3):1959.

[21] Yousaf Z, Bamba K, Bhatti M, Ghafoor U. Charged gravastars in modified gravity. Physical Review D. 2019;100(2):024062.
[22] Del Popolo A, Pace F, Mota DF. Mass-temperature relation in Λ CDM and modified gravity. Physical Review D. 2019;100(2):024013.
[23] Daouda MH, Rodrigues ME, Houndjo M. Reconstruction of f (T) gravity according to holographic dark energy. The European Physical Journal C. 2012;72(2):1893.
[24] Li B, Sotiriou TP, Barrow JD. Large-scale Structure in f (T) Gravity. Physical Review D. 2011;83(10):104017.
[25] Karami K, Abdolmaleki A. Generalized second law of thermodynamics in f (T) gravity. Journal of Cosmology and Astroparticle Physics. 2012;2012(04):007.
[26] Arabsalmani M, Sahni V. Statefinder hierarchy: An extended null diagnostic for concordance cosmology. Physical Review D. 2011;83(4):043501.
[27] Xu L, Lu J, Li W. Generalized holographic and Ricci dark energy models. The European Physical Journal C. 2009;64(1):89.
[28] Gao C, Wu F, Chen X, Shen YG. Holographic dark energy model from Ricci scalar curvature. Physical Review D. 2009;79(4):043511.
[29] Barrow JD, Liddle AR. Perturbation spectra from intermediate inflation. Physical Review D. 1993;47(12):R5219.
[30] Barrow JD, Nunes N. Dynamics of "logamediate" inflation. Physical Review D. 2007;76(4):043501.
[31] Ellis GF, Maartens R. The emergent universe: Inflationary cosmology with no singularity. Classical and Quantum Gravity. 2003;21(1):223.
[32] Mukherjee S, Paul B, Dadhich N, Maharaj S, Beesham A. Emergent universe with exotic matter. Classical and Quantum Gravity. 2006;23(23):6927.
[33] Debnath U, Chattopadhyay S, Jamil M. Fractional action cosmology: some dark energy models in emergent, logamediate, and intermediate scenarios of the universe. Journal of Theoretical and Applied Physics. 2013;7(1):25.
[34] Dkabrowski MP. Statefinders, higher-order energy conditions, and sudden future singularities. Physics Letters B. 2005;625(3-4):184–188.
[35] Macdonald A. Comment on" The Cosmic Time in Terms of the Redshift", by Carmeli et al; 2016. arXiv preprint gr-qc/0606038.
[36] Pasqua A, Assaf KA, Aly AA. Power law and logarithmic entropy corrected Ricci dark energy models in Brans-Dicke chameleon cosmology. International Journal of Theoretical Physics. 2014;53(2):566–578.
[37] Zadeh MA, Sheykhi A. Stability of HDE model with sign-changeable interaction in Brans-Dicke theory; 2018. arXiv preprint arXiv:180410843.
[38] Bekenstein JD. Black holes and entropy. Physical Review D. 1973;7(8):2333.
[39] Iqbal A, Jawad A. Thermodynamics of Ricci-Gauss-Bonnet Dark Energy. Advances in High Energy Physics. 2018;2018.
[40] Azuma K, Subramanian S. Do black holes store negative entropy?; 2018. arXiv preprint arXiv:180706753.

Peer-review history:
The peer review history for this paper can be accessed here:
http://www.sdiarticle4.com/review-history/53138